The Transcription Factor ATF4 Promotes Skeletal Myofiber Atrophy during Fasting

Scott M. Ebert, Alex Mas Monteys, Daniel K. Fox, Kale S. Bongers, Bridget E. Shields, Sharon E. Malmberg, Beverly L. Davidson, Manish Suneja, and Christopher M. Adams

Department of Internal Medicine (C.M.A.), Department of Veterans Affairs Medical Center, Iowa City, Iowa 52246; and Department of Internal Medicine (S.M.E., A.M., D.K.F., K.S.B., B.E.S., S.E.M., B.L.D., M.S., C.M.A.), Roy J. and Lucille A. Carver College of Medicine, The University of Iowa, Iowa City, Iowa 52242

Prolonged fasting alters skeletal muscle gene expression in a manner that promotes myofiber atrophy, but the underlying mechanisms are not fully understood. Here, we examined the potential role of activating transcription factor 4 (ATF4), a transcription factor with an evolutionarily ancient role in the cellular response to starvation. In mouse skeletal muscle, fasting increases the level of *ATF4* mRNA. To determine whether increased ATF4 expression was required for myofiber atrophy, we reduced ATF4 expression with an inhibitory RNA targeting ATF4 and found that it reduced myofiber atrophy during fasting. Likewise, reducing the fasting level of *ATF4* mRNA with a phosphorylation-resistant form of eukaryotic initiation factor 2α decreased myofiber atrophy. To determine whether ATF4 was sufficient to reduce myofiber size, we overexpressed ATF4 and found that it reduced myofiber size in the absence of fasting. In contrast, a transcriptionally inactive ATF4 construct did not reduce myofiber size, suggesting a requirement for ATF4-mediated transcriptional regulation. To begin to determine the mechanism of ATF4-mediated myofiber atrophy, we compared the effects of fasting and ATF4 overexpression on global skeletal muscle mRNA expression. Interestingly, expression of ATF4 increased a small subset of five fasting-responsive mRNAs, including four of the 15 mRNAs most highly induced by fasting. These five mRNAs encode proteins previously implicated in growth suppression ($p21^{Cip1/Waf1}$, GADD45α, and PW1/Peg3) or titin-based stress signaling [muscle LIM protein (MLP) and cardiac ankyrin repeat protein (CARP)]. Taken together, these data identify ATF4 as a novel mediator of skeletal myofiber atrophy during starvation. **(*Molecular Endocrinology* 24: 790–799, 2010)**

Expression of the basic leucine zipper (bZIP) activating transcription factor 4 (ATF4) (also known as CREB-2) is tightly regulated and leads to the activation of many genes involved in the cellular response to stress (1, 2). The best-characterized pathway to ATF4 expression is mediated by phosphorylation of the eukaryotic translation initiation factor 2α (eIF2α) on serine residue 51, which occurs in response to various intracellular stress signals such as depletion of free intracellular amino acids (3–6). eIF2α phosphorylation reduces the amount of eIF2 · GTP · Met-$tRNA_i$ complex required for high levels of mRNA translation initiation. However, eIF2α phosphorylation also increases the level of *ATF4* mRNA and preferentially increases ATF4 synthesis by reducing the inhibitory effects of upstream open reading frames in the *ATF4* transcript. Thus, as a result of eIF2α phosphorylation, global protein synthesis is reduced, but levels of *ATF4* mRNA and ATF4 protein are increased (7, 8).

In mammals, adult skeletal muscle is the principal repository of amino acids and protein, and gross alterations in skeletal muscle amino acid and protein content (reflected as changes in the size of skeletal myofibers) underlie common conditions such as skeletal

ISSN Print 0888-8809 ISSN Online 1944-9917
Printed in U.S.A.

doi: 10.1210/me.2009-0345 Received August 20, 2009. Accepted January 15, 2010.
First Published Online March 2, 2010

Abbreviations: ATF4, Activating transcription factor 4; bZIP, basic leucine zipper; CARP, cardiac ankyrin repeat protein; eGFP, enhanced GFP; eIF2α, eukaryotic translation initiation factor 2α; GFP, green fluorescent protein; MLP, muscle LIM protein; qPCR, quantitative real-time RT-PCR; TA, tibialis anterior.

muscle atrophy. A classical cause of skeletal muscle atrophy is food deprivation, which reduces free intracellular amino acid levels, increases eIF2α phosphorylation, increases *ATF4* mRNA levels, decreases global protein synthesis, and promotes proteolysis and autophagy in skeletal muscle (9–12). However, the consequences of ATF4 expression in skeletal muscle have not been examined. In the current studies, we tested the hypothesis that ATF4 might promote skeletal myofiber atrophy during food deprivation.

Results

ATF4 is required for skeletal myofiber atrophy during fasting

We used quantitative real-time RT-PCR (qPCR) to assess the effect of fasting on *ATF4* mRNA in mouse tibialis anterior (TA) muscle. Relative to levels in nonfasted control mice, skeletal muscle *ATF4* mRNA levels in fasted mice were increased (Fig. 1A). These data are consistent with the results of a previous oligonucleotide microarray study showing that fasting increases the level of *ATF4* mRNA in mouse gastrocnemius muscle (11). With the goal of reducing fasting-mediated ATF4 expression, we inserted a small interfering RNA sequence known to knock down ATF4 expression (13) into the hairpin of a miR-30-based micro-RNA shuttle (14), thereby generating a plasmid encoding miR-ATF4. We then transfected miR-ATF4 plasmid into mouse TA muscles via electroporation. In each mouse, one TA muscle received miR-ATF4 plasmid, and the contralateral TA muscle received an equivalent amount of empty vector. Two weeks later, we subjected the mice to a 24-h fast and then compared *ATF4* mRNA levels between the two TA muscles of each animal. Under nonfasting conditions, miR-ATF4 had little effect on levels of *ATF4* mRNA (Fig. 1B). However, miR-ATF4 prevented the fasting-induced elevation of *ATF4* mRNA (Fig. 1B).

To determine whether ATF4 is required for skeletal myofiber atrophy during fasting, we cotransfected miR-ATF4 plasmid and a plasmid encoding green fluorescent protein (GFP), which served as a transfection marker. Previous studies demonstrated that when a mixture of two plasmids (each expressing a distinct cDNA) is electroporated into skeletal muscle, more than 90% of transfected myofibers coexpress both cDNAs (15, 16). Moreover, transfection of markers such as GFP (Supplemental Fig. 2) or enhanced GFP (eGFP) (17) does not alter myofiber size. Two weeks after transfection, we examined the effect of fasting on the size of transfected myofibers. In the absence of fasting, miR-ATF4 did not significantly alter myofiber size (Fig. 1, C and D). In contrast, under fasting conditions, miR-ATF4 reduced atrophy of transfected myofibers. This was reflected as a rightward shift of the fiber size distribution curve (Fig. 1C) and an increased average

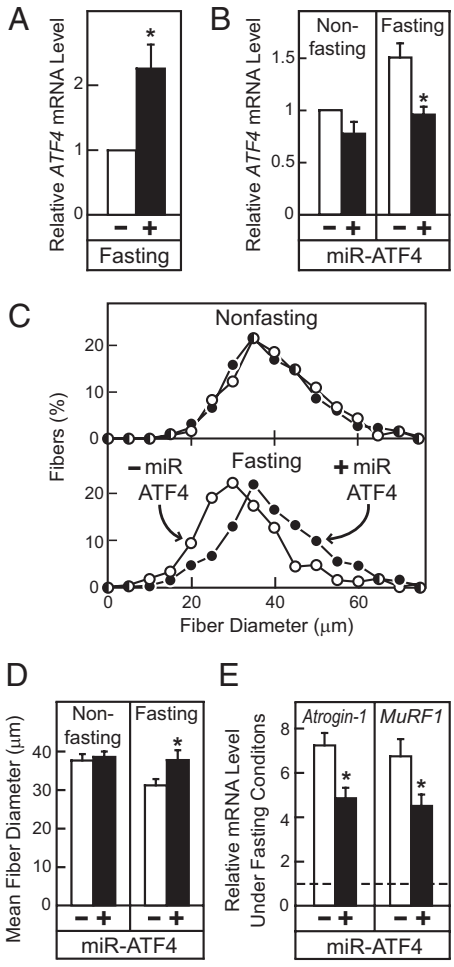

FIG. 1. An artificial micro-RNA targeting ATF4 (miR-ATF4) reduces skeletal muscle *ATF4* mRNA and myofiber atrophy during fasting. A, Mice were allowed *ad libitum* access to food or fasted for 24 h, and then *ATF4* mRNA levels in the TA muscles were determined by qPCR. Data are means ± SEM from four experiments, each using pooled RNA from three mice. *, $P < 0.01$. B–E, Mouse TA muscles were transfected on d 0. On d 14, mice were subjected to nonfasting or fasting conditions for 24 h, as indicated, before the TA muscles were harvested. B, The left TA was transfected with 20 μg empty pU6 vector, and the right TA was transfected with 20 μg pU6-miR-ATF4. TA muscle *ATF4* mRNA levels were determined by qPCR and normalized to levels in the left TA of nonfasted mice. Data are means ± SEM from four experiments and a total of seven transfected muscles per condition. *, $P < 0.02$. C and D, TA muscles were transfected with 5 μg pCMV-GFP plus either 20 μg empty pU6 vector (left TA) or 20 μg pU6-miR-ATF4 (right TA). C, Fiber size distribution curves from a representative experiment. D, Mean diameters of transfected myofibers ± SEM from five experiments each using one mouse. *, $P < 0.01$. E, TA muscles were transfected as described in B. TA muscle mRNA levels were determined by qPCR, and levels under fasting conditions were normalized to levels in TA muscles transfected with empty pU6 vector and harvested under nonfasting conditions, which are indicated by the dashed line. Data are means ± SEM from four experiments and a total of seven transfected muscles per condition. *, $P < 0.02$. Additional micro-RNA controls may be found in Supplemental Fig. 1 (published on The Endocrine Society's Journals Online web site at http://mend.endojournals.org).

myofiber diameter (Fig. 1D). As a biochemical correlate of myofiber atrophy, we examined levels of mRNA transcripts encoding the E3 ubiquitin ligases atrogin-1/MAFbx and MuRF1, which are induced by a broad range of conditions that promote muscle atrophy (18, 19). Figure 1E shows that miR-ATF4 reduced levels of *atrogin-1/MAFbx* and *MuRF1* mRNAs under fasting conditions. These data suggest that increased ATF4 expression is required for skeletal myofiber atrophy during fasting.

eIF2α phosphorylation is known to increase *ATF4* mRNA levels (7, 8), and transfection of cDNA encoding a phosphorylation-resistant form of eIF2α (eIF2α-S51A) inhibits the effects of eIF2α phosphorylation in cultured cell assays (20). Thus, as a second means of reducing ATF4, we transfected TA muscles with plasmid DNA encoding eIF2α-S51A. As in the previous studies, the contralateral TA muscle was transfected with empty vector and served as an intra-subject negative control. Ten days after transfection, we examined the effect of fasting. The immunoblot in Fig. 2A confirmed expression of eIF2α-S51A construct, and Fig. 2B shows that eIF2α-S51A reduced the level of *ATF4* mRNA under fasting conditions. Under nonfasting conditions, eIF2α-S51A did not significantly alter myofiber size (Fig. 2, C and D). However, under fasting conditions, eIF2α-S51A reduced myofiber atrophy (Fig. 2, C and D) as well as levels of *atrogin-1* and *MuRF1* mRNAs (Fig. 2E). These effects of eIF2α-S51A mimicked the effects of miR-ATF4 (Fig. 1) and provide a second line of evidence that increased ATF4 expression is necessary for skeletal myofiber atrophy during fasting.

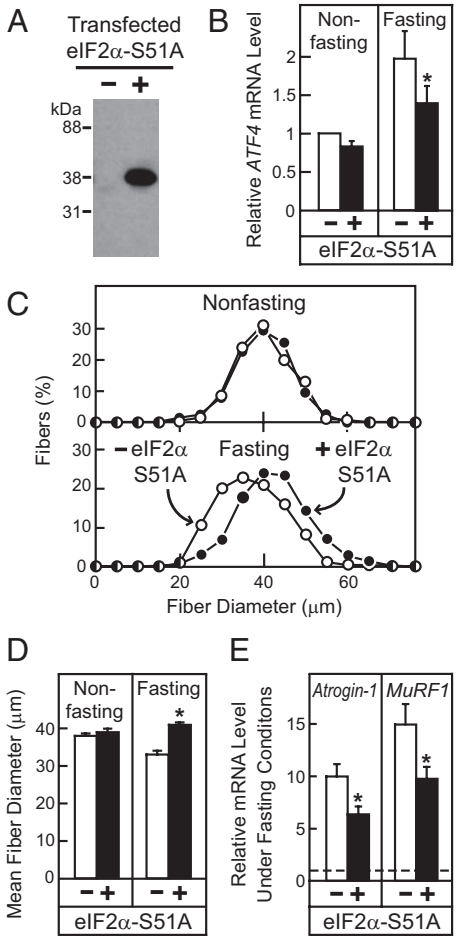

FIG. 2. A phosphorylation-resistant form of eIF2α (eIF2α-S51A) reduces skeletal muscle *ATF4* mRNA and myofiber atrophy during fasting. A–E, Mouse TA muscles were transfected on d 0. On d 10, mice were subjected to nonfasting or fasting conditions for 24 h, as indicated, before the TA muscles were harvested. A and B, The left TA was transfected with 25 μg pcDNA3, and the right TA was transfected with 25 μg pCMV-eIF2α-S51A-FLAG; A, TA muscle protein extracts were subjected to immunoprecipitation with anti-FLAG monoclonal IgG, followed by SDS-PAGE and immunoblot analysis with anti-eIF2α polyclonal antiserum; B, TA muscle *ATF4* mRNA levels were determined by qPCR and normalized to levels in the left TA of nonfasted mice, which were set at 1. Data are means ± SEM from five experiments each using pooled RNA from three mice. *, $P < 0.01$. C and D, Mouse TA muscles were transfected with 2 μg pCMV-eGFP plus either 25 μg pcDNA3 (left TA) or 25 μg pCMV-eIF2α-S51A-FLAG (right TA); C, fiber size distribution curves from a representative experiment; D, mean diameters of transfected myofibers ± SEM from three experiments using a total of seven mice. *, $P < 0.01$. E, TA muscles were transfected as described in A and B. TA muscle mRNA levels were determined by qPCR, and levels under fasting conditions were normalized to levels in TA muscles transfected with pcDNA3 and harvested under nonfasting conditions, which are indicated by the dashed line. Data are means ± SEM from five experiments, each using pooled RNA from three mice. *, $P < 0.01$.

ATF4 overexpression reduces skeletal myofiber size in the absence of fasting

To determine whether ATF4 is sufficient to reduce myofiber size, we transfected TA muscles with plasmid encoding ATF4 and then examined transfected myofibers in the absence of fasting. The immunoblot in Fig. 3A confirmed heterologous expression of ATF4. In the presence of wild-type ATF4, many transfected fibers had the shrunken appearance characteristic of atrophy (Fig. 3B), and the fiber size distribution curve was shifted to the left (Fig. 3C). As expected, ATF4 overexpression was inhibited by miR-ATF4 (Fig. 3D), which shifted the fiber size distribution curve back to the right (Fig. 3E). These data indicate that increased ATF4 expression is sufficient to reduce skeletal myofiber size.

As an additional control, we transfected TA muscles with plasmid encoding a transcriptionally inactive ATF4 construct that contains a series of point mutations in the bZIP domain (ATF4ΔbZIP) (7, 21). The immunoblot in Fig. 4A confirmed expression of the full-length mutant ATF4 construct. Whereas wild-type ATF4 reduced the average diameter of transfected myofibers by more than 25% (Fig. 4C), ATF4ΔbZIP did not

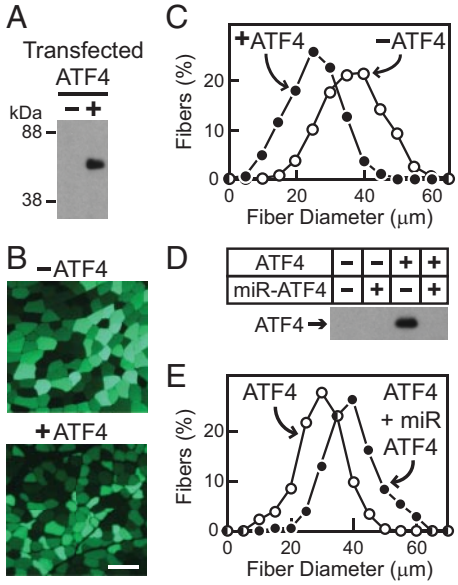

FIG. 3. Overexpression of ATF4 reduces myofiber size in the absence of fasting. A, Mouse TA muscles were transfected with 20 μg empty pcDNA3 vector (left TA) or 20 μg pCMV-ATF4-FLAG (right TA) and then harvested under nonfasting conditions 11 d later. Skeletal muscle protein extracts were subjected to immunoprecipitation with anti-ATF4 polyclonal antiserum, followed by SDS-PAGE and immunoblot analysis with anti-FLAG monoclonal IgG. B and C, Mouse TA muscles were transfected with 5 μg pCMV-GFP plus either 20 μg empty pcDNA3 vector (left TA) or 20 μg pCMV-ATF4-FLAG (right TA) and then harvested under nonfasting conditions 11 d later; B, representative images in the absence or presence of pCMV-ATF4-FLAG (*bar*, 100 μm); C, representative fiber size distribution curves from one of eight experiments. D, Mouse TA muscles were transfected with 15 μg empty pcDNA3 vector or pCMV-ATF4-FLAG with or without 20 μg pU6 vector or pU6-miR-ATF4, as indicated. Muscles were harvested under nonfasting conditions 9 d after transfection, and skeletal muscle protein extracts were analyzed as in A. E, Mouse TA muscles were transfected with 5 μg pCMV-GFP plus 15 μg pCMV-ATF4-FLAG plus either 20 μg pU6 vector (left TA) or 20 μg pU6-miR-ATF4 (right TA) and then harvested under nonfasting conditions 12 d after transfection. Data are representative fiber size distribution curves from one of three experiments.

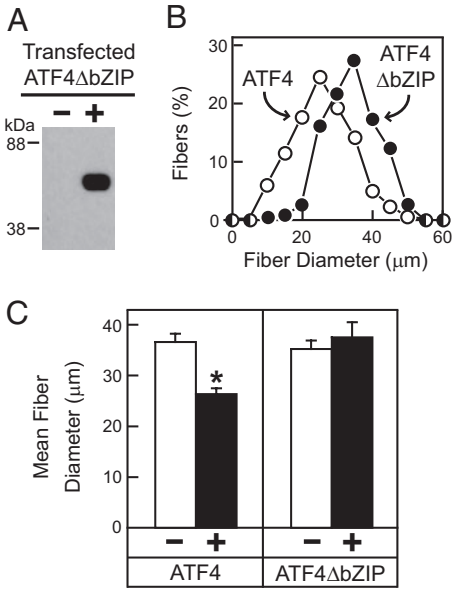

FIG. 4. ATF4-mediated reduction in myofiber size requires an intact bZIP domain. A, Mouse TA muscles were transfected with 20 μg empty pcDNA3 vector (left TA) or 20 μg pCMV-ATF4ΔbZIP-FLAG (right TA) and then harvested under nonfasting conditions 11 d later. Skeletal muscle protein extracts were subjected to immunoprecipitation with anti-ATF4 polyclonal antiserum, followed by SDS-PAGE and immunoblot analysis with anti-FLAG monoclonal IgG. B and C, Left-sided mouse TA muscles were transfected with 5 μg pCMV-GFP plus 20 μg empty pcDNA3 vector. Right-sided TA muscles were transfected with 5 μg pCMV-GFP plus either 20 μg pCMV-ATF4-FLAG or 20 μg pCMV-ATF4ΔbZIP-FLAG, as indicated. Muscles were harvested under nonfasting conditions 11 d later. B, Representative fiber size distribution curves in the presence of pCMV-ATF4-FLAG or pCMV-ATF4ΔbZIP-FLAG from one of six experiments. C, Mean fiber diameters ± SEM from at least six experiments per ATF4 construct. *, $P < 0.01$ using paired *t* tests.

reduce fiber size (Fig. 4, B and C). These results suggest that increased ATF4 expression reduces myofiber size by altering gene expression.

ATF4 overexpression reproduces the effect of fasting on five skeletal muscle mRNAs

To investigate the effects of ATF4 on gene expression, we first examined the effect of ATF4 overexpression on *atrogin-1* and *MuRF1* mRNA levels, which were decreased by both miR-ATF4 and eIF2α-S51A (Figs. 1 and 2). However, in multiple experiments, we were unable to find any evidence of increased *atrogin-1* or *MuRF1* mRNA levels at early or late time points after ATF4 overexpression (Supplemental Fig. 3). Thus, although ATF4 was sufficient to reduce myofiber size (Figs. 3 and 4), it was not sufficient to induce *atrogin-1* and *MuRF1* mRNAs. This suggested that ATF4 might regulate other skeletal muscle mRNAs that were increased or decreased by fasting.

To test this idea, we used exon expression arrays to compare the effects of fasting and ATF4 on global TA muscle mRNA expression. First, to determine the effect of fasting, we compared TA mRNA levels in mice that were subjected to fasting or nonfasting conditions for 24 h. Second, to determine the effect of ATF4, we compared TA mRNA levels in mice whose left TA was transfected with empty plasmid vector and whose right TA was transfected with plasmid encoding ATF4. In both experiments, 16,756 transcripts were measured, and we defined significantly altered mRNAs as those mRNAs whose levels changed by 1.4-fold with a *P* value $\leq$0.01. Compared with ATF4 overexpression, fasting had a broader effect on skeletal muscle mRNA expression, increasing 146 mRNAs and decreasing 100 mRNAs. In contrast, ATF4 overexpression increased 25 mRNAs and decreased three mRNAs. A complete list of mRNAs whose levels were altered by fasting or ATF4 overexpression may be found in Supplemental Tables 1 and 2.

A

mRNA	Protein	Fold Change With Fasting	Fold Change With ATF4
FAM134B	FAM134B	4.8	0.9
FBXO32	Atrogin-1	4.3	0.8
PDK4	Pyruvate Dehydrogenase Kinase-4	3.8	0.9
MT2	Metallothionein 2	3.5	1.0
KLHL38	Kelch-like 38	3.4	0.9
CDKN1A	**p21 / Cip1 / Waf1**	**3.4**	**1.5**
SESN1	Sestrin 1	2.9	0.9
ANKRD2	Ankyrin Repeat Domain Protein 2	2.8	1.1
CSRP3	**Muscle LIM Protein (MLP)**	**2.6**	**1.8**
PEG3	**Peg3 / PW1**	**2.5**	**1.8**
INMT	Indolethylamine N-methyltransferase	2.4	0.8
FKBP5	FK506 Binding Protein 5	2.4	0.8
NPC1	Niemann Pick Type C1	2.4	0.8
PPP1R15A	GADD34	2.4	1.2
GADD45A	**GADD45α**	**2.3**	**1.6**

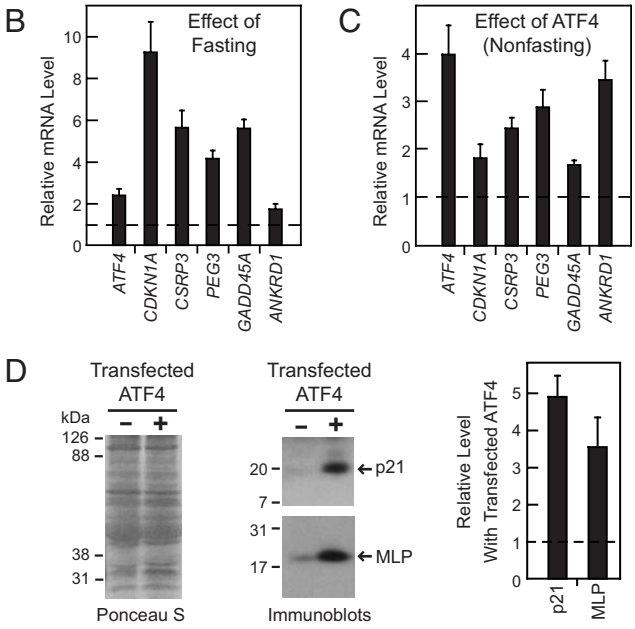

FIG. 5. ATF4 increases a subset of five fasting-responsive skeletal muscle mRNAs. A, To determine the effect of fasting on skeletal muscle mRNA expression, mice were allowed *ad libitum* access to food or fasted for 24 h before TA muscle RNA was harvested. RNA from three mice per group was pooled and then subjected to exon expression array analysis. mRNA levels under fasting conditions were normalized to levels under nonfasting conditions, which were set at 1. To determine the effect of ATF4 overexpression on skeletal muscle mRNA expression, mouse TA muscles were transfected with 25 μg empty pcDNA3 vector (left TA) or 25 μg pCMV-ATF4-FLAG (right TA). TA muscle RNA was harvested under nonfasting conditions 11 d later and then subjected to exon expression array analysis. mRNA levels in the presence of ATF4 (right TA) were normalized to levels in the absence of ATF4 (left TA), which were set at 1. Both experiments were performed four times to generate the final data. The figure shows the 15 mRNAs most increased by fasting as well as the effect of ATF4 on these mRNAs. Data are the mean fold changes induced by fasting or ATF4. For all mRNAs shown, the effect of fasting was statistically significant ($P \leq 0.01$). The *red boldface* denotes transcripts that were also increased by ATF4 ($P \leq 0.01$). B, Mice were subjected to nonfasting or fasting conditions for 24 h, and then TA muscle mRNA was harvested and analyzed by qPCR. mRNA levels under fasting conditions were normalized to mRNA levels under nonfasting conditions, which were set at 1 and are indicated by the *dashed line*. Data are the means ± SEM from four experiments. $P \leq 0.03$ for all mRNAs shown. C and D, Mouse TA muscles were transfected with 25 μg empty pcDNA3 vector (left TA) or 25 μg pCMV-ATF4-FLAG (right TA). TA muscles were harvested under nonfasting conditions 11 d later. C, TA muscle mRNA was analyzed by qPCR. mRNA levels in the presence of ATF4 (right TA) were normalized to mRNA levels in the absence of ATF4 (left TA), which were set at 1 and are indicated by the *dashed line*. Data are the means ± SEM from seven experiments. $P \leq 0.01$ for all mRNAs shown. D, An equal amount (100 μg) of total muscle protein extract from each condition was subjected to SDS-PAGE, followed by immunoblot analysis with anti-p21 monoclonal IgG or anti-MLP polyclonal antiserum. The membranes were stained with Ponceau S to confirm equal sample loading. The graph shows average densitometry signals ± SEM from three experiments. Levels in the presence of ATF4 (right TA) were normalized to levels in the absence of ATF4 (left TA), which were set at 1 and are indicated by the *dashed line*.

By comparing mRNAs that were altered by fasting with mRNAs that were altered by ATF4, we identified five mRNAs that were significantly increased by both conditions: *CDKN1A* (encoding $p21^{Cip1/Waf1}$), *CSRP3* [encoding muscle LIM protein (MLP)], *PEG3* (encoding PW1/Peg3), *GADD45A* (encoding GADD45α), and *ANKRD1* [encoding cardiac ankyrin repeat protein (CARP)]. Interestingly, four of these mRNAs (*CDKN1A*, *CSRP3*, *PEG3*, and *GADD45A*) were among the 15 mRNAs most highly increased by fasting (Fig. 5A).

We used qPCR to confirm fasting- and ATF4-mediated increases in these five mRNAs. As predicted by the exon expression arrays, fasting and ATF4 increased levels of *CDKN1A*, *CSRP3*, *PEG3*, *GADD45A*, and *ANKRD1* mRNAs (Fig. 5, B and C). To determine whether the ATF4-mediated increase in *CDKN1A* and *CSRP3* mRNAs led to increased levels of p21 and MLP, we performed immunoblot analysis of total skeletal muscle protein extracts in the absence or presence of ATF4 overexpression. Figure 5D shows that ATF4 increased p21 and MLP protein levels by more than 3-fold. These data suggest that ATF4 promotes myofiber atrophy by inducing a small but important subset of fasting-responsive genes.

Discussion

ATF4 is an evolutionarily ancient regulator of amino acid and protein metabolism and the cellular response to stress (1–4, 7, 8), but its effects in skeletal muscle were not known. In the current studies, we found that fasting increased the level of skeletal muscle *ATF4* mRNA, which in turn was required for atrophy of skeletal myofibers. Moreover, increased ATF4 expression reduced myofiber size in the absence of fasting. These data identify ATF4 as a

novel, inducible mediator of skeletal myofiber atrophy during starvation.

We also found that a phosphorylation-resistant eIF2α construct (eIF2α-S51A) reduced *ATF4* mRNA and myofiber atrophy under fasting conditions. This result suggests that fasting increases ATF4 expression via eIF2α phosphorylation and is consistent with a recent report of increased skeletal muscle eIF2α phosphorylation during food deprivation (10). The downstream mechanisms of ATF4-dependent atrophy appear to be complex. ATF4 is a bZIP transcription factor capable of activating or repressing genes in a cell-type-specific manner (22). Our data indicate that an intact bZIP domain is required for ATF4-mediated atrophy and that ATF4 functions primarily as a transcriptional activator in skeletal muscle.

Interestingly, when we reduced ATF4 levels with miR-ATF4 or eIF2α-S51A, it reduced fasting-mediated induction of mRNAs encoding atrogin-1 and MuRF1, which catalyze proteolytic events during skeletal muscle atrophy (19, 23–26). However, ATF4 was not sufficient to increase *atrogin-1* or *MuRF1* mRNAs, suggesting an alternate mechanism for ATF4-mediated myofiber atrophy. Indeed, by comparing global mRNA expression profiles induced by fasting or ATF4 overexpression, we identified five mRNAs (*CDKN1A*, *GADD45A*, *PEG3*, *CSRP3*, and *ANKRD1*) that were highly induced by both conditions. These data suggest the hypothesis that ATF4 reduces myofiber size by increasing expression of *CDKN1A*, *GADD45A*, *PEG3*, *CSRP3*, and *ANKRD1* mRNAs.

We do not yet know whether these five mRNAs are necessary for fasting-mediated myofiber atrophy or whether they are sufficient to induce myofiber atrophy in the absence of fasting. However, there is some evidence that they might be involved. *CDKN1A* and *GADD45A* mRNAs encode well-described inhibitors of cellular growth ($p21^{Cip1/Waf1}$ and GADD45α, respectively) (27–29), and *PEG3* mRNA encodes a protein required for cancer cachexia (PW1/Peg3) (30). *CSRP3* and *ANKRD1* mRNAs encode proteins that are thought to mediate titin-based stress signaling from the sarcomere to the nucleus (MLP and CARP, respectively) (31). Both MLP and CARP have the capacity to translocate to the nucleus and alter gene transcription (32, 33) but are also found in myofibrils, where they may play structural roles at their specific binding sites within the sarcomere (the Z-line and the I-band for MLP and CARP, respectively) (34, 35). Interestingly, a recent study found that MLP interacts with cofilin 2 at the Z-disc and facilitates cofilin 2-mediated actin filament depolymerization, suggesting that induction of MLP might a play direct role in myofibril disassembly (36). Determining the roles of $p21^{Cip1/Waf1}$, GADD45α, PW1/Peg3, MLP, and CARP in fasting-mediated myofiber atrophy is an important area for future investigation.

Skeletal muscle atrophy is a nearly universal consequence of illness and aging; however, we still lack targeted medical therapies to prevent or reverse it. The current studies focused on the role of skeletal muscle ATF4 during starvation, but previous work associated increased skeletal muscle eIF2α phosphorylation with cancer cachexia (37) and increased skeletal muscle *ATF4* mRNA levels with cancer cachexia, insulin deficiency, uremia, and muscle denervation (18). Large increases in skeletal muscle *CSRP3*, *ANKRD1*, *CDKN1A*, and *GADD45A* mRNA levels have been observed after muscle denervation (32, 38, 39), and skeletal muscle *ANKRD1* and *CSRP3* mRNA levels are increased by insulin deficiency (40). Furthermore, *CDKN1A*, *GADD45A*, and *PEG3* mRNAs are increased in age-related sarcopenia (41–43). These considerations suggest that the induction of ATF4 may have a generalized role in the pathogenesis of skeletal muscle atrophy. Further investigations of this possibility may suggest new therapeutic approaches for this common and debilitating condition.

Materials and Methods

Plasmids

The coding region of mouse ATF4 (NM_009716) was amplified from mouse L cell cDNA and then cloned into p3XFLAG-CMV10 (Sigma Chemical Co., St. Louis, MO) to place three copies of the FLAG epitope tag at the NH_3 terminus and generate pCMV-ATF4-FLAG. pCMV-ATF4 (ΔbZIP)-FLAG was generated by site-directed mutagenesis of pCMV-ATF4-FLAG, substituting ^{292}GLYEAAA^{298} for ^{292}RYRQKKR^{298}. pU6-miR-ATF4 was generated by first using polymerase extension of overlapping DNA oligonucleotides to insert the antisense sequence 5′-TTAAACTAAAGGAATGCTCTG-3′ into a human miR-30-based micro-RNA shuttle (14) and then cloning this micro-RNA shuttle into the pU6 vector, which consists of a mouse U6 promoter, a multiple cloning site, and an RNA polymerase III terminator sequence in the TOPO-BluntII vector (Invitrogen, Carlsbad, CA). The antisense sequence encoded by miR-ATF4 is complementary to mouse ATF4 but is not complementary to other mRNAs described in these studies. Moreover, the seed region of miR-ATF4 does not show complementarity to other mRNAs described in these studies. Human FLAG epitope-tagged eIF2α-S51A was generously provided by Dr. Glen N. Barber (20) and subcloned into pcDNA3 to generate pCMV-eIF2α-S51A-FLAG. pCMV-GFP and pCMV-eGFP were pcDNA3 encoding GFP or eGFP, respectively.

Mouse muscle transfection

All studies described in this manuscript used male C57BL/6 mice that were obtained from the National Cancer Institute at

ages 6–8 wk and used for experiments within 3 wk of their arrival. One advantage of the adult mouse TA muscle as an experimental system is that it can be readily transfected with plasmid DNA via electroporation. Electroporation transfects nuclei of terminally differentiated adult myofibers, but not nuclei of satellite cells or connective tissue cells (44), and has been used to study several proteins that regulate adult skeletal myofiber physiology and morphology (15, 23, 25, 44–54). In our hands, plasmid DNA expression occurs in approximately 40% of TA myofibers and is maintained for more than 3 wk after transfection. Before transfection, mice were anesthetized by an ip injection of 91 mg/kg ketamine and 9.1 mg/kg xylazine, after which the hind limbs were shaved with a straight razor, and the TA muscles were injected with 30 μl hyaluronidase solution (which was prepared by resuspending bovine placental hyaluronidase (Sigma) in sterile injectable 0.9% NaCl at a concentration of 0.4 U/μl). Two hours later, the mice were reanesthetized, and TA muscles were injected with plasmid DNA (which was prepared using endotoxin-free plasmid purification kits (QIAGEN, Valencia, CA) and resuspended in sterile injectable 0.9% NaCl at a concentration of 1 μg/μl). All TA muscle injections used a 30-gauge needle inserted 2 mm into the distal end of the TA muscle (at a 10° angle to the long axis of the muscle). After injection of plasmid DNA, the hind limbs were placed between two-paddle electrodes and subjected to 10 pulses (20 msec) of 175 V/cm (with 480-msec intervals between pulses) using an ECM-830 electroporator (BTX Harvard Apparatus, Holliston, MA). All animal procedures were approved by the Institutional Animal Care and Use Committee of the University of Iowa.

Analysis of protein levels

After harvest, mouse TA muscles were snap frozen in liquid N_2 and homogenized in 1 ml ice-cold lysis buffer [50 mM Tris (pH 7.4), 150 mM NaCl, 1% (vol/vol) Triton X-100, 1.5 mM $MgCl_2$, 1 mM sodium EDTA, 1 mM sodium EGTA, 25 μg/ml *N*-acetyl-leucinal-leucinal-norleucinal (ALLN), 1 μg/ml pepstatin A, 2 μg/ml aprotonin, 10 μg/ml leupeptin, 200 μM phenylmethylsulfonyl fluoride, 640 μM benzamidine, and a 1:100 dilution of phosphatase inhibitor cocktail 1 (Sigma)] using a polytron (Tissue Master 240; Omni International, Kennesaw, GA) for 1 min on setting no. 8. The homogenate was rotated at 4 C for 1 h to generate a total muscle protein extract. In experiments involving eIF2α-S51A-FLAG, ATF4-FLAG, and ATF4ΔbZIP-FLAG, we were unable to detect the heterologously expressed proteins by SDS-PAGE of total muscle protein extract, and thus we performed immunoprecipitations as follows: the total muscle protein extract was centrifuged at 4 C and 16,000 × *g* for 20 min to generate a Triton X-100 soluble protein extract. The protein concentration of this Triton X-100 soluble extract was measured using the BCA kit (Pierce, Rockford, IL), after which the extract was diluted to a concentration of 3 mg/ml in ice-cold lysis buffer (final volume 500 μl). We then added 2 μg anti-FLAG mouse monoclonal antibody (Sigma) or 2 μg rabbit anti-ATF4 polyclonal antiserum (Santa Cruz Biotechnology, Santa Cruz, CA) plus 50 μl protein G plus Sepharose beads (Santa Cruz) and rotated the samples at 4 C for 16 h. Immunoprecipitates were washed three times for 20 min with 1 ml lysis buffer and then mixed with 100 μl 1× sample buffer [50 mM Tris-HCl (pH 6.8), 2% SDS, 5% glycerol, 0.04% (wt/vol) bromophenol blue] containing 5% (wt/vol) 2-mercaptoethanol and heated for 5 min at 95 C. Immunoprecipitates were subjected to 10% SDS-PAGE (for eIF2α) or 8% SDS-PAGE (for ATF4) and then transferred to Hybond-C extra nitrocellulose filters (Millipore, Billerica, MA). Immunoblots were performed at room temperature using a 1:1000 dilution of rabbit anti-eIF2α polyclonal antiserum (Cell Signaling, Danvers, MA) or a 1:1500 dilution of mouse anti-FLAG monoclonal antibody (Sigma). To assess p21 and MLP protein levels, the protein concentration of total muscle protein extract was measured with the BCA kit, after which an aliquot was mixed with 0.25 vol 5× sample buffer [250 mM Tris-HCl (pH 6.8), 10% SDS, 25% glycerol, 0.2% (wt/vol) bromophenol blue] containing 5% (wt/vol) 2-mercaptoethanol and heated for 5 min at 95 C. An equal amount of protein from each sample (100 μg) was subjected to 10% SDS-PAGE and then transferred to Hybond-C extra nitrocellulose filters. Immunoblots were performed at 4 C for 16 h using a 1:750 dilution of mouse anti-p21 monoclonal IgG (Sigma) or a 1:1000 dilution of chicken anti-MLP polyclonal antiserum (Abcam, Cambridge, MA).

Skeletal muscle mRNA analysis by qPCR

After harvest, muscle samples were immediately placed in RNAlater (Ambion, Austin, TX). Total RNA was extracted using TRIzol solution (Invitrogen) and then treated with deoxyribonuclease I using the Turbo DNA-*free* kit (Ambion). First-strand cDNA was synthesized in a 100-μl reaction that contained 2 μg RNA, random hexamer primers, and components of the TaqMan reverse transcription kit (Applied Biosystems, Foster City, CA). Levels of *ATF4*, *MuRF1*, and *atrogin-1* mRNAs were measured using oligonucleotide primers (Supplemental Table 3) that were designed using Primer Express software (Applied Biosystems). For these studies, the real-time PCR contained, in a final volume of 20 μl, 20 ng reverse-transcribed RNA, 167 nM forward and reverse primers, and 10 μl Power SYBR Green PCR Master Mix (Applied Biosystems). Levels of *CDKN1A*, *GADD45A, PEG3, CSRP3*, and *ANKRD1* mRNAs were measured using mouse TaqMan Gene Expression Assays (Applied Biosystems), and the real-time PCR contained, in a final volume of 20 μl, 20 ng reverse-transcribed RNA, 1 μl 20× TaqMan Gene Expression Assay, and 10 μl TaqMan Gene Expression Master Mix. qPCR was carried out using a 7500 Fast Real-Time PCR System (Applied Biosystems). All qPCR were performed in triplicate, and the cycle threshold (Ct) values were averaged to give the final results. To analyze the data, we used the ΔCt method, with level of *36B4* mRNA serving as the invariant control, and used *t* tests to determine statistical significance.

Histological analysis

After harvest, TA muscles were immediately placed in 4% (wt/vol) paraformaldehyde at 4 C for 16 h and then moved to 30% (wt/vol) sucrose solution at 4 C for at least 24 h. The middle of the muscle belly was then cut transversely with a straight razor and embedded in tissue freezing medium, after which 10-μm sections from the midbelly were prepared using a Microm HM 505 E cryostat equipped with a CryoJane sectioning system (Instrumedics, Richmond, IL). Sections were mounted with Vectashield mounting medium (Vector Laboratories, Burlingame, CA) and examined on an Olympus IX-71 microscope equipped with a DP-70 camera and a GFP-specific epifluorescence filter. Image analysis was performed using

ImageJ software, and transfected fibers were defined as fibers with a mean fluorescence of 25 or more arbitrary units. In each experiment, we measured the diameter of at least 200 transfected myofibers per muscle, using the lesser diameter method described elsewhere (55), and used paired *t* tests to compare the results from bilateral TA muscles of each animal.

Microarray analysis of skeletal muscle mRNA levels

After harvest, muscles were immediately placed in RNAlater (Ambion) and stored at −80 C until further use. Total RNA was extracted using TRIzol solution (Invitrogen) according to the manufacturer's instructions. Microarray hybridizations were performed at the University of Iowa DNA Facility. Briefly, 50 ng total RNA was converted to SPIA amplified cDNA using the WT-Ovation Pico RNA Amplification System, version 1 (NuGEN Technologies, San Carlos, CA; catalog no. 3300) according to the manufacturer's recommended protocol. The amplified SPIA cDNA product was purified through a QIAGEN MinElute Reaction Cleanup column (QIAGEN; catalog no. 28204) according to modifications from NuGEN. Four micrograms of SPIA amplified DNA were used to generate ST-cDNA using the WT-Ovation Exon Module version 1 (NuGEN Technologies; catalog no. 2000) and again cleaned up with the QIAGEN column as above. Five micrograms of this product were fragmented (average fragment size = 85 bases) and biotin labeled using the NuGEN FL-Ovation cDNA Biotin Module, version 2 (NuGEN Technologies; catalog no. 4200) per the manufacturer's recommended protocol. The resulting biotin-labeled cDNA was mixed with Affymetrix eukaryotic hybridization buffer (Affymetrix, Inc., Santa Clara, CA), placed onto Mouse Exon 1.0 ST arrays, and incubated at 45 C for 18 h with 60 rpm rotation in an Affymetrix Model 640 Genechip Hybridization Oven. After hybridization, the arrays were washed, stained with streptavidin-phycoerythrin (Molecular Probes, Inc., Eugene, OR), signal amplified with antistreptavidin antibody (Vector) using the Affymetrix Model 450 Fluidics Station. Arrays were scanned with the Affymetrix Model 3000 scanner with 7G upgrade, and data were collected using the GeneChip operating software (GCOS) version 1.4. In Mouse Exon 1.0 ST arrays, the log2 hybridization signal reflects the mean signal intensity of all exon probes specific for an individual mRNA and is proportional to the level of that mRNA. To determine which mRNAs were present at a significantly different level ($P \leq 0.01$), we used paired *t* tests to compare log2 hybridization signals (between samples in the absence or presence of fasting or between samples transfected in the absence or presence of ATF4 transfection) and then applied a secondary requirement of a 1.4-fold change. To restrict our analysis to those mRNAs with reasonably high levels of expression, we excluded mRNAs that were not increased to a mean log2 hybridization signal of at least 5 or decreased from a mean log2 hybridization signal of at least 5. All raw microarray data have been deposited in Gene Expression Omnibus (GEO, accession number GSE 20104).

Acknowledgments

We thank Drs. Michael Welsh, Peter Snyder, Jennifer Stern, and Steven Kunkel for invaluable discussions and critical review of the manuscript. We also thank Tammy Lisi and Heather Lei for excellent technical assistance, Tom Moninger and Chantal Allamargot of the University of Iowa Central Microscopy Core Facility for assistance with microscopy, and Thomas Bair of the University of Iowa DNA Facility for assistance with the microarray analysis.

Address all correspondence and requests for reprints to: Christopher M. Adams or Manish Suneja, Department of Internal Medicine, Roy J. and Lucille A. Carver College of Medicine, The University of Iowa, Iowa City, Iowa 52242. E-mail: christopher-adams@uiowa.edu or manish-suneja@uiowa.edu.

This work was supported by a Career Development Award from the Department of Veterans Affairs, Veterans Health Administration, Office of Research and Development, and a Junior Faculty Award from the American Diabetes Association (to C.M.A.), a Predoctoral Fellowship in Molecular and Cellular Biology (NIH T32 GM073610 to S.M.E.), the University of Iowa Medical Scientist Training Program (D.K.F. and K.S.B.), and the University of Iowa Summer Undergraduate Medical Scientist Training Program (B.E.S.).

Disclosure Summary: The authors have nothing to disclose.

References

1. **Harding HP, Zhang Y, Zeng H, Novoa I, Lu PD, Calfon M, Sadri N, Yun C, Popko B, Paules R, Stojdl DF, Bell JC, Hettmann T, Leiden JM, Ron D** 2003 An integrated stress response regulates amino acid metabolism and resistance to oxidative stress. Mol Cell 11:619–633
2. **Yamaguchi S, Ishihara H, Yamada T, Tamura A, Usui M, Tominaga R, Munakata Y, Satake C, Katagiri H, Tashiro F, Aburatani H, Tsukiyama-Kohara K, Miyazaki J, Sonenberg N, Oka Y** 2008 ATF4-mediated induction of 4E-BP1 contributes to pancreatic β-cell survival under endoplasmic reticulum stress. Cell Metab 7:269–276
3. **Wek RC, Cavener DR** 2007 Translational control and the unfolded protein response. Antioxid Redox Signal 9:2357–2371
4. **Proud CG** 2005 eIF2 and the control of cell physiology. Semin Cell Dev Biol 16:3–12
5. **Kaufman RJ, Davies MV, Pathak VK, Hershey JW** 1989 The phosphorylation state of eucaryotic initiation factor 2 alters translational efficiency of specific mRNAs. Mol Cell Biol 9:946–958
6. **Pathak VK, Schindler D, Hershey JW** 1988 Generation of a mutant form of protein synthesis initiation factor eIF-2 lacking the site of phosphorylation by eIF-2 kinases. Mol Cell Biol 8:993–995
7. **Siu F, Bain PJ, LeBlanc-Chaffin R, Chen H, Kilberg MS** 2002 ATF4 is a mediator of the nutrient-sensing response pathway that activates the human asparagine synthetase gene. J Biol Chem 277:24120–24127
8. **Hinnebusch AG** 2005 Translational regulation of GCN4 and the general amino acid control of yeast. Annu Rev Microbiol 59:407–450
9. **Hammarqvist F, Andersson K, Luo JL, Wernerman J** 2005 Free amino acid and glutathione concentrations in muscle during short-term starvation and refeeding. Clin Nutr 24:236–243
10. **Yuan CL, Sharma N, Gilge DA, Stanley WC, Li Y, Hatzoglou M, Previs SF** 2008 Preserved protein synthesis in the heart in response to acute fasting and chronic food restriction despite reductions in liver and skeletal muscle. Am J Physiol Endocrinol Metab 295: E216–E222
11. **Jagoe RT, Lecker SH, Gomes M, Goldberg AL** 2002 Patterns of gene expression in atrophying skeletal muscles: response to food deprivation. FASEB J 16:1697–1712
12. **Sandri M** 2008 Signaling in muscle atrophy and hypertrophy. Physiology (Bethesda) 23:160–170
13. **Adams CM** 2007 Role of the transcription factor ATF4 in the anabolic actions of insulin and the anti-anabolic actions of glucocorticoids. J Biol Chem 282:16744–16753

14. **Boudreau RL, Monteys AM, Davidson BL** 2008 Minimizing variables among hairpin-based RNAi vectors reveals the potency of shRNAs. RNA 14:1834–1844
15. **Alzghoul MB, Gerrard D, Watkins BA, Hannon K** 2004 Ectopic expression of IGF-I and Shh by skeletal muscle inhibits disuse-mediated skeletal muscle atrophy and bone osteopenia in vivo. FASEB J 18:221–223
16. **Rana ZA, Ekmark M, Gundersen K** 2004 Coexpression after electroporation of plasmid mixtures into muscle in vivo. Acta Physiol Scand 181:233–238
17. **Judge AR, Koncarevic A, Hunter RB, Liou HC, Jackman RW, Kandarian SC** 2007 Role for IκBα, but not c-Rel, in skeletal muscle atrophy. Am J Physiol 292:C372–382
18. **Sacheck JM, Hyatt JP, Raffaello A, Jagoe RT, Roy RR, Edgerton VR, Lecker SH, Goldberg AL** 2007 Rapid disuse and denervation atrophy involve transcriptional changes similar to those of muscle wasting during systemic diseases. FASEB J 21:140–155
19. **Bodine SC, Latres E, Baumhueter S, Lai VK, Nunez L, Clarke BA, Poueymirou WT, Panaro FJ, Na E, Dharmarajan K, Pan ZQ, Valenzuela DM, DeChiara TM, Stitt TN, Yancopoulos GD, Glass DJ** 2001 Identification of ubiquitin ligases required for skeletal muscle atrophy. Science 294:1704–1708
20. **Perkins DJ, Barber GN** 2004 Defects in translational regulation mediated by the alpha subunit of eukaryotic initiation factor 2 inhibit antiviral activity and facilitate the malignant transformation of human fibroblasts. Mol Cell Biol 24:2025–2040
21. **He CH, Gong P, Hu B, Stewart D, Choi ME, Choi AM, Alam J** 2001 Identification of activating transcription factor 4 (ATF4) as an Nrf2-interacting protein. Implication for heme oxygenase-1 gene regulation. J Biol Chem 276:20858–20865
22. **Hai T, Hartman MG** 2001 The molecular biology and nomenclature of the activating transcription factor/cAMP responsive element binding family of transcription factors: activating transcription factor proteins and homeostasis. Gene 273:1–11
23. **Lagirand-Cantaloube J, Offner N, Csibi A, Leibovitch MP, Batonnet-Pichon S, Tintignac LA, Segura CT, Leibovitch SA** 2008 The initiation factor eIF3-f is a major target for atrogin1/MAFbx function in skeletal muscle atrophy. EMBO J 27:1266–1276
24. **Clarke BA, Drujan D, Willis MS, Murphy LO, Corpina RA, Burova E, Rakhilin SV, Stitt TN, Patterson C, Latres E, Glass DJ** 2007 The E3 Ligase MuRF1 degrades myosin heavy chain protein in dexamethasone-treated skeletal muscle. Cell Metab 6:376–385
25. **Lagirand-Cantaloube J, Cornille K, Csibi A, Batonnet-Pichon S, Leibovitch MP, Leibovitch SA** 2009 Inhibition of atrogin-1/MAFbx mediated MyoD proteolysis prevents skeletal muscle atrophy in vivo. PloS One 4:e4973
26. **Cohen S, Brault JJ, Gygi SP, Glass DJ, Valenzuela DM, Gartner C, Latres E, Goldberg AL** 2009 During muscle atrophy, thick, but not thin, filament components are degraded by MuRF1-dependent ubiquitylation. J Cell Biol 185:1083–1095
27. **el-Deiry WS, Tokino T, Velculescu VE, Levy DB, Parsons R, Trent JM, Lin D, Mercer WE, Kinzler KW, Vogelstein B** 1993 WAF1, a potential mediator of p53 tumor suppression. Cell 75:817–825
28. **Harper JW, Adami GR, Wei N, Keyomarsi K, Elledge SJ** 1993 The p21 Cdk-interacting protein Cip1 is a potent inhibitor of G1 cyclin-dependent kinases. Cell 75:805–816
29. **Rosemary Siafakas A, Richardson DR** 2009 Growth arrest and DNA damage-45α (GADD45α). Int J Biochem Cell Biol 41:986–989
30. **Schwarzkopf M, Coletti D, Sassoon D, Marazzi G** 2006 Muscle cachexia is regulated by a p53-PW1/Peg3-dependent pathway. Genes Dev 20:3440–3452
31. **Granzier HL, Labeit S** 2004 The giant protein titin: a major player in myocardial mechanics, signaling, and disease. Circ Res 94:284–295
32. **Arber S, Halder G, Caroni P** 1994 Muscle LIM protein, a novel essential regulator of myogenesis, promotes myogenic differentiation. Cell 79:221–231
33. **Zou Y, Evans S, Chen J, Kuo HC, Harvey RP, Chien KR** 1997 CARP, a cardiac ankyrin repeat protein, is downstream in the Nkx2-5 homeobox gene pathway. Development 124:793–804
34 **Knöll R, Hoshijima M, Hoffman HM, Person V, Lorenzen-Schmidt I, Bang ML, Hayashi T, Shiga N, Yasukawa H, Schaper W, McKenna W, Yokoyama M, Schork NJ, Omens JH, McCulloch AD, Kimura A, Gregorio CC, Poller W, Schaper J, Schultheiss HP, Chien KR** 2002 The cardiac mechanical stretch sensor machinery involves a Z disc complex that is defective in a subset of human dilated cardiomyopathy. Cell 111:943–955
35. **Miller MK, Bang ML, Witt CC, Labeit D, Trombitas C, Watanabe K, Granzier H, McElhinny AS, Gregorio CC, Labeit S** 2003 The muscle ankyrin repeat proteins: CARP, ankrd2/Arpp and DARP as a family of titin filament-based stress response molecules. J Mol Biol 333:951–964
36. **Papalouka V, Arvanitis DA, Vafiadaki E, Mavroidis M, Papadodima SA, Spiliopoulou CA, Kremastinos DT, Kranias EG, Sanoudou D** 2009 Muscle LIM protein interacts with cofilin 2 and regulates F-actin dynamics in cardiac and skeletal muscle. Mol Cell Biol 29:6046–6058
37. **Eley HL, Skipworth RJ, Deans DA, Fearon KC, Tisdale MJ** 2008 Increased expression of phosphorylated forms of RNA-dependent protein kinase and eukaryotic initiation factor 2α may signal skeletal muscle atrophy in weight-losing cancer patients. Br J Cancer 98:443–449
38. **Laure L, Suel L, Roudaut C, Bourg N, Ouali A, Bartoli M, Richard I, Danièle N** 2009 Cardiac ankyrin repeat protein is a marker of skeletal muscle pathological remodelling. FEBS J 276:669–684
39. **Zeman RJ, Zhao J, Zhang Y, Zhao W, Wen X, Wu Y, Pan J, Bauman WA, Cardozo C** 2009 Differential skeletal muscle gene expression after upper or lower motor neuron transection. Pflugers Arch 458:525–535
40. **Lehti TM, Silvennoinen M, Kivelä R, Kainulainen H, Komulainen J** 2007 Effects of streptozotocin-induced diabetes and physical training on gene expression of titin-based stretch-sensing complexes in mouse striated muscle. Am J Physiol Endocrinol Metab 292:E533–E542
41. **Edwards MG, Anderson RM, Yuan M, Kendziorski CM, Weindruch R, Prolla TA** 2007 Gene expression profiling of aging reveals activation of a p53-mediated transcriptional program. BMC Genomics 8:80
42. **Welle S, Brooks AI, Delehanty JM, Needler N, Thornton CA** 2003 Gene expression profile of aging in human muscle. Physiol Genomics 14:149–159
43. **Welle S, Brooks AI, Delehanty JM, Needler N, Bhatt K, Shah B, Thornton CA** 2004 Skeletal muscle gene expression profiles in 20–29 year old and 65–71 year old women. Exp Gerontol 39:369–377
44. **Sartori R, Milan G, Patron M, Mammucari C, Blaauw B, Abraham R, Sandri M** 2009 Smad2 and 3 transcription factors control muscle mass in adulthood. Am J Physiol Cell Physiol 296:C1248–C1257
45. **Sandri M, Sandri C, Gilbert A, Skurk C, Calabria E, Picard A, Walsh K, Schiaffino S, Lecker SH, Goldberg AL** 2004 Foxo transcription factors induce the atrophy-related ubiquitin ligase atrogin-1 and cause skeletal muscle atrophy. Cell 117:399–412
46. **Van Gammeren D, Damrauer JS, Jackman RW, Kandarian SC** 2009 The IκB kinases IKKα and IKKβ are necessary and sufficient for skeletal muscle atrophy. FASEB J 23:362–370
47. **Durieux AC, Amirouche A, Banzet S, Koulmann N, Bonnefoy R, Pasdeloup M, Mouret C, Bigard X, Peinnequin A, Freyssenet D** 2007 Ectopic expression of myostatin induces atrophy of adult skeletal muscle by decreasing muscle gene expression. Endocrinology 148:3140–3147
48. **Pallafacchina G, Calabria E, Serrano AL, Kalhovde JM, Schiaffino S** 2002 A protein kinase B-dependent and rapamycin-sensitive pathway controls skeletal muscle growth but not fiber type specification. Proc Natl Acad Sci USA 99:9213–9218
49. **Senf SM, Dodd SL, McClung JM, Judge AR** 2008 Hsp70 overex-

pression inhibits NF-κB and Foxo3a transcriptional activities and prevents skeletal muscle atrophy. FASEB J 22:3836–3845

50. **Murgia M, Serrano AL, Calabria E, Pallafacchina G, Lomo T, Schiaffino S** 2000 Ras is involved in nerve-activity-dependent regulation of muscle genes. Nat Cell Biol 2:142–147
51. **Bodine SC, Stitt TN, Gonzalez M, Kline WO, Stover GL, Bauerlein R, Zlotchenko E, Scrimgeour A, Lawrence JC, Glass DJ, Yancopoulos GD** 2001 Akt/mTOR pathway is a crucial regulator of skeletal muscle hypertrophy and can prevent muscle atrophy in vivo. Nat Cell Biol 3:1014–1019
52. **Dobrowolny G, Aucello M, Rizzuto E, Beccafico S, Mammucari C, Boncompagni S, Bonconpagni S, Belia S, Wannenes F, Nicoletti C, Del Prete Z, Rosenthal N, Molinaro M, Protasi F, Fanò G, Sandri M, Musarò A** 2008 Skeletal muscle is a primary target of SOD1G93A-mediated toxicity. Cell Metab 8:425–436
53. **Sandri M, Lin J, Handschin C, Yang W, Arany ZP, Lecker SH, Goldberg AL, Spiegelman BM** 2006 PGC-1α protects skeletal muscle from atrophy by suppressing FoxO3 action and atrophy-specific gene transcription. Proc Natl Acad Sci USA 103:16260–16265
54. **Mammucari C, Milan G, Romanello V, Masiero E, Rudolf R, Del Piccolo P, Burden SJ, Di Lisi R, Sandri C, Zhao J, Goldberg AL, Schiaffino S, Sandri M** 2007 FoxO3 controls autophagy in skeletal muscle in vivo. Cell Metab 6:458–471
55. **Dubowitz V, Lane R, Sewry CA** 2007 Muscle biopsy : a practical approach. 3rd ed. Philadelphia: Saunders Elsevier